 doi:10.20944/preprints202106.0139.v1

Type of the Paper (Communication.)

Prediction of biometric variables through multispectral images obtained from UAV in beans (*Phaseolus vulgaris* L.) during ripening stage

Javier Quille-Mamani [1*], Rossana Porras-Jorge [1], David Saravia-Navarro [1,2], Jordán Herrera[1], Julio Chavez-Galarza [1], Carlos I. Arbizu [1]

[1] Dirección de Desarrollo Tecnológico Agrario, Instituto Nacional de Innovación Agraria (INIA), Av. La Molina 1981, Lima 15024, Lima, Perú; R. P-J. (riego_tecnificado@inia.gob.pe); D.S.-N. (agricultura_precision@inia.gob.pe); J.H. (jordanhf13@gmail.com); J. Ch-G. (jcchavezgalarza@gmail.com); C.I.A. (carbizu@inia.gob.pe)

[2] Facultad de Agronomía, Universidad Nacional Agraria La Molina, Av. La Molina s/n, Lima 15024, Lima, Lima Perú.

* Correspondence: geomatica@inia.gob.pe; +51 945189689

Abstract: Here, we report the prediction of vegetative stages variables of canary bean crop by means of RGB and multispectral images obtained from UAV during the ripening stage, correlating the vegetation indices with biometric variables measured manually in the field. Results indicated a highly significant correlation of plant height with eight RGB image vegetation indices for the canary bean crop, which were used for predictive models, obtaining a maximum correlation of $R^2 = 0.79$. On the other hand, the estimated indices of multispectral images did not show significant correlations.

Keywords: Vegetation indices; precision agriculture; RGB images

1. Introduction

Bean (*Phaseolus vulgaris* L.) is a legume with a protein content of 20 to 25% and 50 to 60% carbohydrates, and is part of the human diet worldwide, mainly in developing countries [1]. It is widely cultivated for its enormous genetic diversity, it is a nitrogen-fixing plant, highly adaptable and productive in a wide range of environments [2, 3]. This crop will likely play a key role in guaranteeing food security for millions of people around the world in the near future [4]. In Peru in 2019, a total of 73,298 ha of beans were cultivated, representing 0.8% of the Gross Value of Agricultural Production (GVaP) [5]. Canary beans is the most outstanding cultivar in the Peruvian coast due to its preference in the national diet, and cultural aspects. Therefore, due to the importance of this crop, it is a great challenge to monitor its development together with an appropriate agronomic management in the field [6] in the context of climate change.

Quantitative evaluations of biometric variables such as plant height, leaf area index, and chlorophyll content influence yield and are becoming a high priority under precision agriculture [7]. Efficient and non-destructive monitoring of crop growth is essential for accurate crop management and is key to digital agriculture [8]. Determining data manually requires a significant amount of time and resources (measuring equipment, reagents, and researchers, among others). To increase agricultural production with limited resources, important technological advances have been implemented such as the use of unmanned aerial vehicles (UAVs) [9].

UAVs are tools that provide new alternatives of monitoring crops, without direct contact on them [10], allowing the prediction of crop development in a spatial-temporal way. The sensors coupled to a UAV allow estimating vegetative development variables

 doi:10.20944/preprints202106.0139.v1

with different vegetative indices [11]. Recently, in the north of China, [12] used UAV images to predict yield in corn crop. Similarly, other researchers, predicted aerial biomass in various crops such as sunflower, corn and wheat [13–16]. Similarly, in Kenya RGB images were used to estimate growth and nutritional yield of cassava [17]. Since evaluations are necessary during the development of crops and as beans are one of the main foods in the basic family basket, it is essential that research is conducted to guarantee food security under the context of climate change. Therefore, the objective of the present work was to estimate the prediction of plant height, chlorophyll content and leaf area index through multispectral images obtained from UAV of canary bean crop during the ripening stage.

2. Materials and Methods

2.1. Study site

The study site is located in the research field of the National Institute of Agrarian Innovation (INIA for its acronym in Spanish) (12°4'30.10"S, 76 ° 56'33.86"W, 240 masl) (Figure 1). The experiment was developed during the winter-spring seasons (Jun 26-Oct 20, 2020), using commercial canary beans. This research was conducted in an experimental field of 0.30 ha (Figure 2) with distances between plants and rows of 0.2 m and 0.9 m, respectively. We used drip irrigation with a distance between drippers of 0.2 m with a flow of 1.20 l/h. The study site is arid according to the climatic classification of Warren Thornthwaitees [18], recording for the year 2020 averages of 76.8% RH, wind speed 3.3m/s and temperature 19.2 °C (Figure 1), and a total annual rainfall of 8 mm. The meteorological data was recorded from an automatic station (VANTAGE Pro2 Plus Davis, California, USA), located at the Alexander Von Humbolt meteorological observatory of the La Molina National Agrarian University at a distance of 0.87 km from the research area.

2.2. Field data collection

Three biometric variables were recorded on 16 plots of 7m x 5m at 90, 97 and 101 days after sowing (DAS):

- Plant height (cm); it was measured manually from the soil surface to the highest stem apex.
- Leaf area index (LAI); it was estimated from digital images taken on the canopy cover of the plant on a 0.2m x 0.9m frame. Image processing was performed with the Green CropTracker software (v. 1.0, Agriculture and Agri-Food Canada) using a histogram-based threshold method according to [19].
- Chlorophyll content (mg / m2); it was measured with the CCM-300 equipment (Opti-Sciences Hudson, NH, USA) following the methodologies of [20] choosing leaves from the upper third free of mechanical and biotic damage.

2.3. *UAV RGB and multispectral image acquisition and processing*

We used a Quadcopter type UAV platform, DJI Phantom 4 Pro (Shenzhen Dajiang Baiwang Technology Co., Ltd., Shenzhen, China) with a built-in 4864 × 3648 pixel resolution RGB camera. In addition, a multispectral sensor Parrot Sequoia (Parrot SA, France) which is a synchronized array of 4 single-band multispectral camera with 1.2 MP global shutter was attached, taking images in green (550 nm), red (660 nm), red edge (735 nm) and near infrared (790 nm).

The images were collected at 90, 97 and 101 DAS during sunny days with wind speeds lower than 12 m/s, from 11:00 to 13:00 hours approximately on the 16 research plots, as detailed in Figure 2. The flight plan was established with the Pix4Dcapture software (v. 4.12.1, Pix4D SA, Prilly, Switzerland), considering a frontal and lateral overlap of

Preprints (www.preprints.org) | NOT PEER-REVIEWED | Posted: 4 June 2021 doi:10.20944/preprints202106.0139.v1

80%, height of 30 m, speed of 2.8 m/s and the camera focused at nadir position (perpendicular to the ground surface), allowing to obtain a resolution of 0.8 cm and 2.5 cm for RGB and multispectral images, respectively.

Figure 3 shows a flow chart for data acquisition from UAV platform to image processing. Image processing was performed with Pix4Dmapper Pro software (v. 4.3.33, Pix4D SA, Prilly, Switzerland), according to the following steps: (i) alignment of geolocated images, (ii) generation of point clouds and geometric correction, and (iii) generation of the digital surface and orthomosaic model using the inverse distance weighting method. The geometric correction was performed considering nine ground control points (GCP) (Figure 2) previously installed and registered with differential GNSS (Global Navigation Satellite System) (South Galaxy G1 model, South Surveying & Mapping Instrument Co. Ltd, Guangdong, China).

2.4. *Calculation of vegetation indices*

The calculation of the vegetation indices from RGB images was carried out after to a normalization of the bands (R = red, G = green and B = blue) in the Pix4Dmapper software. In addition, the multispectral bands were obtained (R = red, G = green, RE = red border and NIR = near infrared). In this research, 19 vegetation indices were estimated to assess biometric parameters (Table 1)

2.5. *Statistical analysis*

We recorded the quantitative data (plant height, leaf area index and chlorophyll content) in a field book for the 16 plots and were then analyzed with the R v software. 4.1.0 [21] with the following packages: GGALLI v. 2.0.0 [22], Hmisc v. 4.5-0 [23]. In addition, we employed R base codes to correlate variables evaluated in the field with those estimated through vegetation indices. Statistical indicators such as the Pearson correlation coefficient (r) and determination coefficient (R^2) were determined. Moreover, a principal component analysis was performed with libraries factoextra v.1.0.7 [24] and FactoMiner v.2.4 [25].

3. Results

3.1. *Principal component analysis*

The principal component analysis (PCA) (Figure 4) defined the interactions between the variables evaluated in the field (plant height, leaf area index and chlorine-row content.) with the vegetation indices (19 in total) monitored by UAV with a cumulative variance of 80.6% for the first two dimensions. In addition, PCA generated differentiated clusters between 90 and 97 DAS. However, the last evaluation (101 DAS) did not report a significant difference, indicating that during ripening stage, these variables in the bean crop show minimal rates of increase.

The PCA variables on the axis of dimension 1 that contribute to the variance represent an approximate of 5% in each one. We can also observe that the multispectral indices were greater at 90 DAS as well as the chlorophyll content (Figure 4).

3.2. Correlation between spectral indices and growth variables

The correlation analysis between the vegetation indices and growth variables were carried out for 90, 97 and 101 DAS, finding significant correlations (*p-value* <0.05) at 97 DAS for plant height. In contrast, the other variables (chlorophyll content and leaf area index) did not register significant correlations, so we decided not to consider them for the multiple linear regression model.

Plant height is an important variable since it depends on the growth rate of crops [26]. In Table 2, 19 vegetation indices correlated to plant height are detailed. Four indices (RGBVI, VDVI, ExGR and ExB) presented high significance (*p-value* <0.01), eight indices

 doi:10.20944/preprints202106.0139.v1

(ExR, GBDI, NGBDI, NGRDI, MGRVI, VARI, CRRI and RGRI) showed significance (*p-Value* <0.05), and four indices (ExB, ExR, IKAW and ExG) were inversely proportional. Of the total of evaluated indices, no multispectral index presented significant correlations (NDVI, SAVI, GNDVI and NDREI).

3.2. Prediction model for estimating plant height

After correlating the vegetation indices and plant height at 97 DAS, multiple linear regression analyzes were performed for three prediction models, as detailed in Table 3. Figure 5 shows the three prediction models for the measured plant height and its predicted values: (i) for model I, 10 vegetation indices were used (RGBVI, GBDI, VDVI, NGBDI, NGRDI, MGRVI, VARI, ExGR, CRRI, RGRI) with significant correlations 0.59 < r <0.64, (*p-value* <0.05), generating a predictive model with an $R^2 = 0.79$ (*p-value* <0.01), (ii) in model II four vegetation indices were considered (RGBVI, GBDI, VDVI, ExGR) with significant correlations of 0.63 <r <0.64, (*p-value* <0.01), obtaining a predictive model with $R^2 = 0.60$, and (iii) to generate the prediction model III, three vegetation indices were considered (ExR, ExG, ExB) with negative correlations -0.66 <r<-0.32, generating a predictive model with an $R^2 = 0.46$. Although for model II four vegetation indices with high correlation values were chosen, their prediction decreases due to the fact that it presents an R^2 lower than model I but higher than that of model III.

3.3. Figures, Tables and Schemes

Preprints (www.preprints.org) | NOT PEER-REVIEWED | Posted: 4 June 2021 doi:10.20944/preprints202106.0139.v1

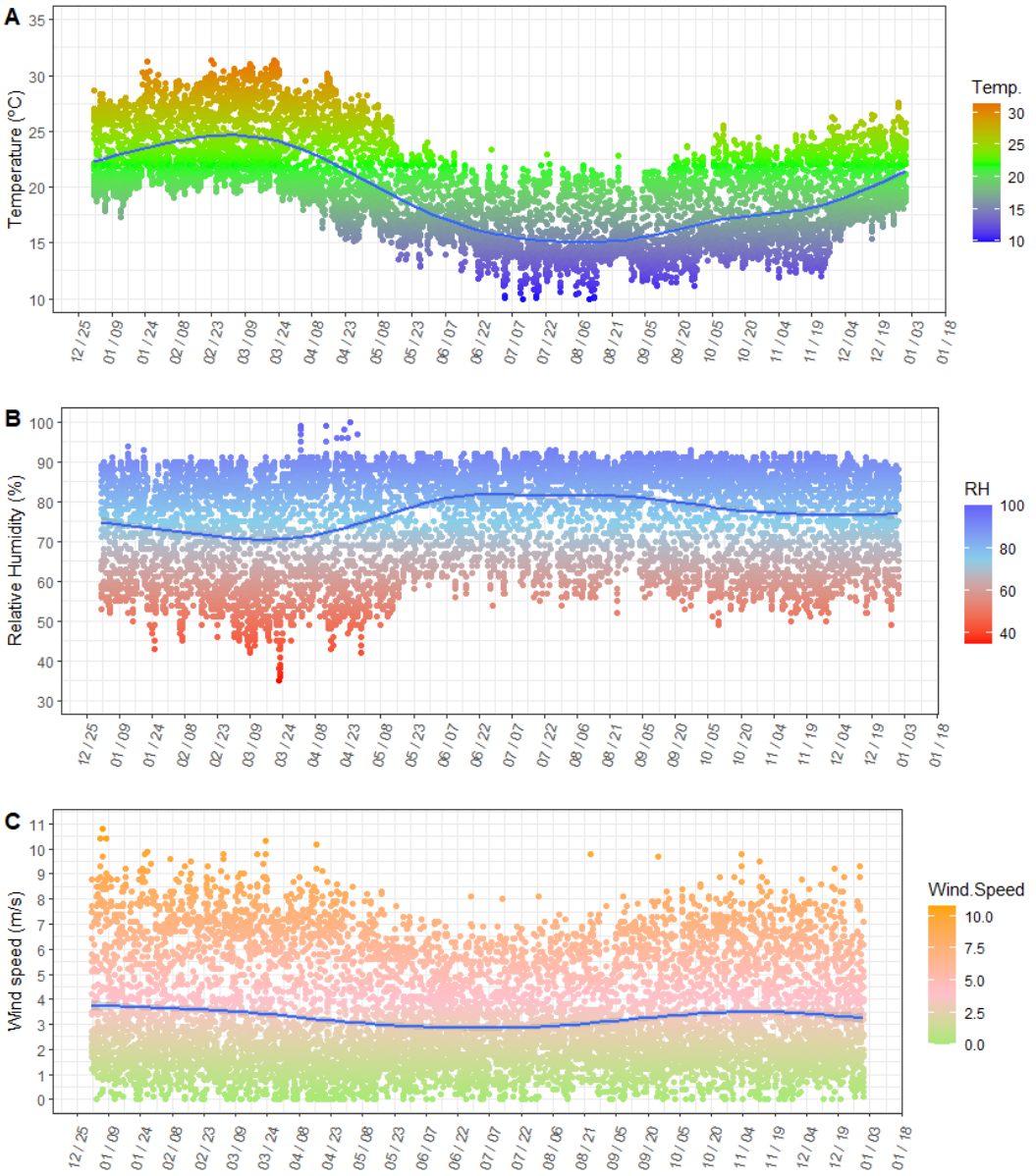

Figure 1. Meteorological data for year 2020 recorded hourly. A) temperature (°C), B) relative humidity (%) and C) wind speed (m / s). The blue line represents the daily average.

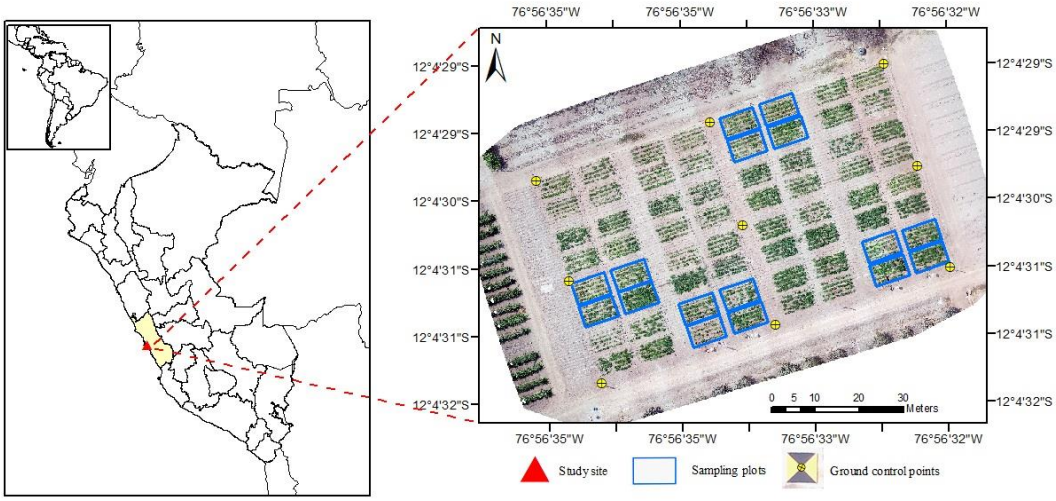

Preprints (www.preprints.org) | NOT PEER-REVIEWED | Posted: 4 June 2021 doi:10.20944/preprints202106.0139.v1

Figure 2. Location of the 64 canary type bean cultivation plots. The ground control points (GCP) are shown, and the 16 plots sampled for the estimation of vegetation indices are shown in blue rectangles.

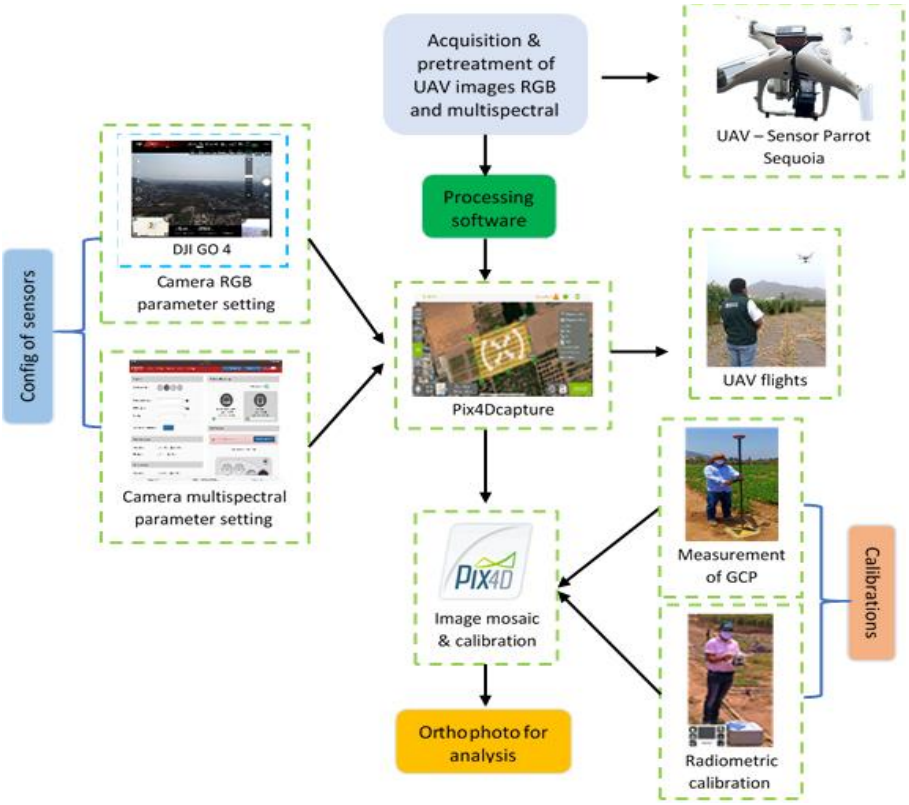

Figure 3. Flowchart for the acquisition and processing of images for the calculation of the vegetation indices of a canary type bean crop.

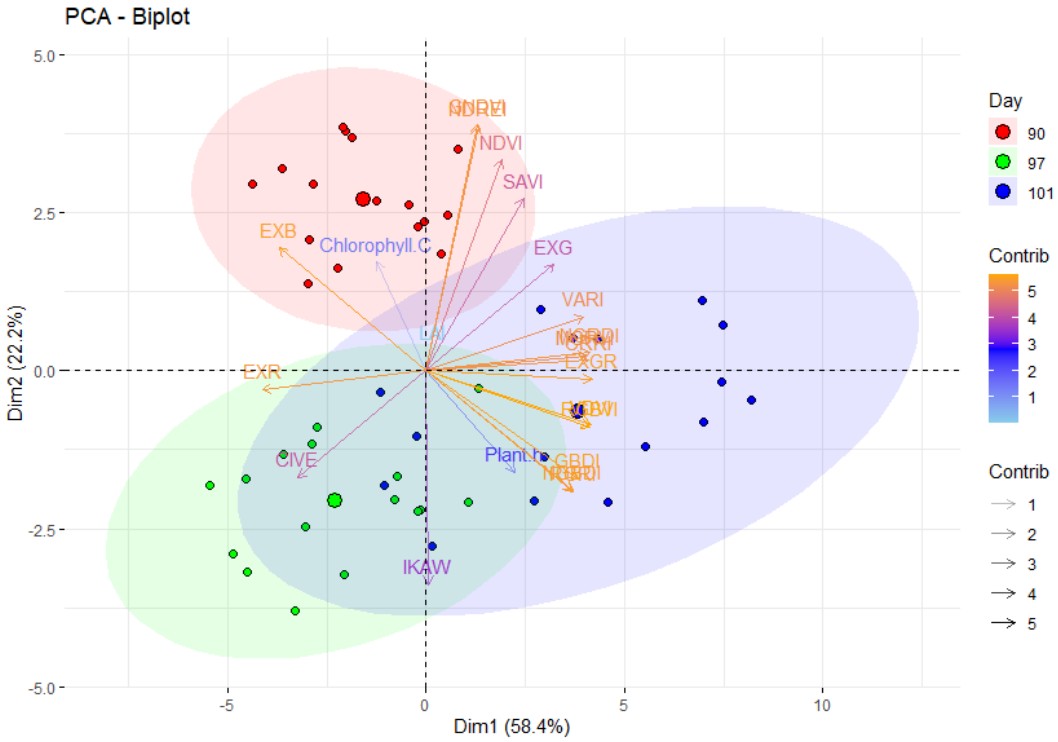

Figure 4. Principal component analysis of growth variables and vegetative indices during ripening stage of canary type bean crop.

Preprints (www.preprints.org) | NOT PEER-REVIEWED | Posted: 4 June 2021 doi:10.20944/preprints202106.0139.v1

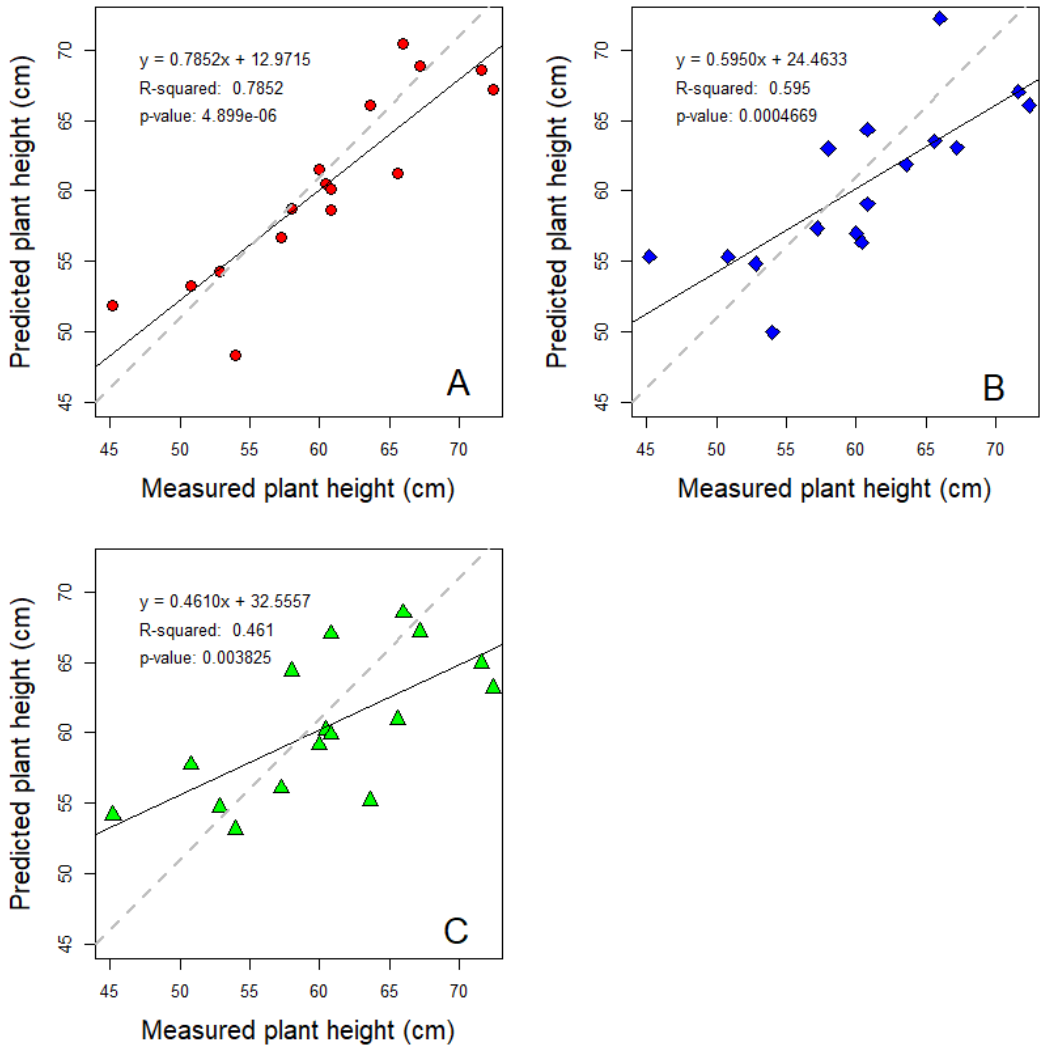

Figure 5. Correlation between the estimated data and plant height recorded for three models, A) Model I is based on ten vegetation indices, B) Model II is based on four vegetation indices, and C) Model III is based on three vegetation indices with inverse correlation.

Table 1. Vegetation index calculations from Red-Green-Blue and Multispectral images

Abbrev	Definition	type	Reference
NGRDI	(G - R)/(G + R)	RGB	[27, 28]
IKAW	(R − B)/(R + B)		[28]
ExR	1.4xR− G		[29]
ExB	1.4xB − G		[29, 30, 31]
ExG	2xG-R-B		[32]
CRRI	G/R		[32, 28]
ExGR	ExG − ExR		[20]
GBDI	G-B		[33]
MGRVI	(G x G-R x R)/(G x G x R x R)		[34]
NGBDI	(G - B)/(G + B)		[35, 36]

Preprints (www.preprints.org) | NOT PEER-REVIEWED | Posted: 4 June 2021 doi:10.20944/preprints202106.0139.v1

RGBVI	(G x G - B x R)/(G x G + B x R)		[36, 37]
VDVI	(2 x G - R -B)/(2 x G + R +B)		[27]
RGRI	R/G		[38]
VARI	(G − R)/(G + R − B)		[39]
CIVE	(0.441 x R - 0.8818 xG + 0.385 x B + 18.787)		[35]
NDVI	(NIR − r)/(NIR + r)	Multiespectral	[40]
GNDVI	(NIR − g)/(NIR + g)		[41]
SAVI	[(NIR − r)/(NIR + r+L)](1+L)		[42]
NDREI	(NIR − re)/(NIR + re)		[43]

Table 2. Vegetation index correlated with plant height recorded at 97 DAS.

Index	**Plant height**		
	***r* Pearson**	***p-value***	
NDVI	0.39	0.135	ns
SAVI	0.40	0.125	ns
GNDVI	0.33	0.215	ns
NDREI	0.37	0.156	ns
CIVE	0.22	0.418	ns
RGBVI	0.64	0.008	**
ExR	-0.62	0.011	*
GBDI	0.63	0.010	*
VDVI	0.64	0.007	**
NGBDI	0.60	0.014	*
NGRDI	0.61	0.011	*
MGRVI	0.61	0.012	*
IKAW	-0.18	0.502	ns
VARI	0.59	0.017	*
ExGR	0.63	0.009	**
ExG	-0.32	0.223	ns
CRRI	0.62	0.010	*
RGRI	0.60	0.014	*
ExB	-0.66	0.005	**

Table 3. Multivariate linear regression models between vegetation indices and plant height recorded during ripening stage for canary bean.

Prediction model	**Spectral Index**	**Regression Coefficient**	**Intercept**	**Model R^2**
I	RGBVI	-2893.1	5934.9	0.79

Preprints (www.preprints.org) | NOT PEER-REVIEWED | Posted: 4 June 2021 doi:10.20944/preprints202106.0139.v1

	GBDI	21228.7		
	VDVI	5500.7		
	NGBDI	- 8715.3		
	NGRDI	5934.9		
	MGRVI	-9715.4		
	VARI	3526.0		
	EXGR	- 5071.7		
	CRRI	- 139.1		
	RGRI	1657.0		
II	RGBVI	- 3556	2709	0.60
	GBDI	4832		
	VDVI	-1332		
	EXGR	- 3179		
III	EXR	-91.31	51.45	0.46
	EXG	210		
	EXB	- 216.05		

4. Discussion and conclusions

To our best knowledge, this is the first research work in Peru using technology such as UAV for an agronomic monitoring of canary beans. A highly significant correlation for plant height was obtained from eight estimated vegetation indices from RGB images in the canary bean crop at ripening stage. It was possible to predict the height of this crop with high performance (R^2 = 0.79) using model I. Recent studies [2, 17] reported similar results for beans and cassava crops, respectively, demonstrating the utility of UAVs and vegetation indices for the compilation of biometric variables. The use of these tools becomes more important due to the need to conduct more agronomic evaluations in a timely manner in crops and mainly in those that are cultivated in arid environments such as the Peruvian coast. We are currently conducting experiments with new technologies using remote sensors such as UAV for the prediction of biometric variables estimated from vegetative indices obtained from RGB and multispectral images in bean crops and others of national importance. In addition, images from the PeruSat-1 (Peru) and Kompsat 3 (South Korea) satellites will be used, allowing timely monitoring and prediction of crop development under different agronomic management scenarios (irrigation, fertilization, among others) on a larger scale.

Author Contributions: Conceptualization and methodology, J.Q.-M.; data analysis and methodology, D.S.-N.; R. P.-J.; writing and revision, D.S.-N.; J. Ch.-G.; C.I.A; J.H.

Funding: PIP 2281955 "Installation of the agricultural technology research service specialized in climate change for the agricultural sector" and PIP 2449640 "Creation of the precision agriculture service in the departments of Lambayeque, Huancavelica, Ucayali and San Martín 4 Departments"

Acknowledgments: We are grateful to PIPs 2281955 and 2449640 for providing funding. Likewise, thanks to the students of the Agrotechnology Research Circle (CIATEC for its acronym in Spanish) of the Faculty of Agronomy, La Molina National Agrarian University for their support during field evaluations.

Conflicts of Interest: The authors declare no conflict of interest

References

1. Campos-Vega, R.; Reynoso-Camacho, R.; Pedraza-Aboytes, G.; Acosta-Gallegos, J. A.; Guzman-Maldonado, S. H.; Paredes-Lopez, O.; Oomah, B. D.; Loarca-Piña, G. Chemical Composition and In Vitro Polysaccharide Fermentation of Different Beans (*Phaseolus Vulgaris* L.). *Journal of Food Science* **2009**, *74* (7), T59–T65. https://doi.org/10.1111/j.1750-3841.2009.01292.x.
2. Parker, T. A.; Palkovic, A.; Gepts, P. Determining the Genetic Control of Common Bean Early-Growth Rate Using Unmanned Aerial Vehicles. *Remote Sensing* **2020**, *12* (11), 1748. https://doi.org/10.3390/rs12111748.
3. Shamseldin, A.; Velázquez, E. The Promiscuity of *Phaseolus Vulgaris* L. (Common Bean) for Nodulation with Rhizobia: A Review. *World J Microbiol Biotechnol* **2020**, *36* (5), 1–12. https://doi.org/10.1007/s11274-020-02839-w.
4. Mecha, E.; Figueira, M. E.; Bronze, M. C. V. P. and M. do R. *Two Sides of the Same Coin: The Impact of Grain Legumes on Human Health: Common Bean (Phaseolus Vulgaris L.) as a Case Study*; IntechOpen, 2018. https://doi.org/10.5772/intechopen.78737.
5. MIDAGRI, D. "Plan Nacional de Cultivos: Campaña Agrícola 2019-2020", https://cdn.www.gob.pe/uploads/document/file/471867/Plan_Nacional_de_Cultivos_2019_2020b.pdf (accessed Mar 28, 2021).
6. Shakoor, N.; Lee, S.; Mockler, T. C. High Throughput Phenotyping to Accelerate Crop Breeding and Monitoring of Diseases in the Field. *Current Opinion in Plant Biology* **2017**, *38*, 184–192. https://doi.org/10.1016/j.pbi.2017.05.006.
7. Eggen, M.; Ozdogan, M.; Zaitchik, B.; Ademe, D.; Foltz, J.; Simane, B. Vulnerability of Sorghum Production to Extreme, Sub-Seasonal Weather under Climate Change. *Environ. Res. Lett.* **2019**, *14* (4), 045005. https://doi.org/10.1088/1748-9326/aafe19.
8. Wang, Y.; Zhang, K.; Tang, C.; Cao, Q.; Tian, Y.; Zhu, Y.; Cao, W.; Liu, X. Estimation of Rice Growth Parameters Based on Linear Mixed-Effect Model Using Multispectral Images from Fixed-Wing Unmanned Aerial Vehicles. *Remote Sensing* **2019**, *11* (11), 1371. https://doi.org/10.3390/rs11111371.
9. Khan, N.; Ray, R. L.; Sargani, G. R.; Ihtisham, M.; Khayyam, M.; Ismail, S. Current Progress and Future Prospects of Agriculture Technology: Gateway to Sustainable Agriculture. *Sustainability* **2021**, *13* (9), 4883. https://doi.org/10.3390/su13094883.
10. Qi, H.; Zhu, B.; Wu, Z.; Liang, Y.; Li, J.; Wang, L.; Chen, T.; Lan, Y.; Zhang, L. Estimation of Peanut Leaf Area Index from Unmanned Aerial Vehicle Multispectral Images. *Sensors* **2020**, *20* (23), 6732. https://doi.org/10.3390/s20236732.
11. Gano, B.; Dembele, J. S. B.; Ndour, A.; Luquet, D.; Beurier, G.; Diouf, D.; Audebert, A. Using UAV Borne, Multi-Spectral Imaging for the Field Phenotyping of Shoot Biomass, Leaf Area Index and Height of West African Sorghum Varieties under Two Contrasted Water Conditions. *Agronomy* **2021**, *11* (5), 850. https://doi.org/10.3390/agronomy11050850.
12. Guo, Y.; Wang, H.; Wu, Z.; Wang, S.; Sun, H.; Senthilnath, J.; Wang, J.; Robin Bryant, C.; Fu, Y. Modified Red Blue Vegetation Index for Chlorophyll Estimation and Yield Prediction of Maize from Visible Images Captured by UAV. *Sensors* **2020**, *20* (18), 5055. https://doi.org/10.3390/s20185055.
13. Han, L.; Yang, G.; Dai, H.; Xu, B.; Yang, H.; Feng, H.; Li, Z.; Yang, X. Modeling Maize Above-Ground Biomass Based on Machine Learning Approaches Using UAV Remote-Sensing Data. *Plant Methods* **2019**, *15* (1), 10. https://doi.org/10.1186/s13007-019-0394-z.
14. Li, W.; Niu, Z.; Chen, H.; Li, D.; Wu, M.; Zhao, W. Remote Estimation of Canopy Height and Aboveground Biomass of Maize Using High-Resolution Stereo Images from a Low-Cost Unmanned Aerial Vehicle System. *Ecological Indicators* **2016**, *67*, 637–648. https://doi.org/10.1016/j.ecolind.2016.03.036.
15. Vega, F. A.; Ramírez, F. C.; Saiz, M. P.; Rosúa, F. O. Multi-Temporal Imaging Using an Unmanned Aerial Vehicle for Monitoring a Sunflower Crop. *Biosystems Engineering* **2015**, *132*, 19–27. https://doi.org/10.1016/j.biosystemseng.2015.01.008.
16. Yue, J.; Feng, H.; Jin, X.; Yuan, H.; Li, Z.; Zhou, C.; Yang, G.; Tian, Q. A Comparison of Crop Parameters Estimation Using Images from UAV-Mounted Snapshot Hyperspectral Sensor and High-Definition Digital Camera. *Remote Sensing* **2018**, *10* (7), 1138. https://doi.org/10.3390/rs10071138.
17. Wasonga, D. O.; Yaw, A.; Kleemola, J.; Alakukku, L.; Mäkelä, P. S. A. Red-Green-Blue and Multispectral Imaging as Potential Tools for Estimating Growth and Nutritional Performance of Cassava under Deficit Irrigation and Potassium Fertigation. *Remote Sensing* **2021**, *13* (4), 598. https://doi.org/10.3390/rs13040598.
18. SENAMHI. Mapa Climático del Perú https://www.senamhi.gob.pe/?&p=mapa-climatico-del-peru.
19. Liu, J.; Pattey, E.; Admiral, S. Assessment of in Situ Crop LAI Measurement Using Unidirectional View Digital Photography. *Agricultural and Forest Meteorology* **2013**, *169*, 25–34. https://doi.org/10.1016/j.agrformet.2012.10.009.
20. Gitelson, A. A.; Kaufman, Y. J.; Stark, R.; Rundquist, D. Novel Algorithms for Remote Estimation of Vegetation Fraction. *Remote Sensing of Environment* **2002**, *80* (1), 76–87. https://doi.org/10.1016/S0034-4257(01)00289-9.
21. R Core Team. RStudio: Integrated Development Environment para R , Boston, MA : RStudio, Inc. http://www.rstudio.com/.
22. Schloerke, B.; Cook, D.; Larmarange, J.; Briatte, F.; Marbach, M.; Thoen, E.; Elberg, A.; Toomet, O.; Crowley, J.; Hofmann, H.; Wickham, H. GGally: Extension to "Ggplot2," 2020.
23. Harrell, F. E. Package 'Hmisc,' 2021.
24. Kassambara, A.; Mundt, F. "factoextra: Extract and Visualize the Results of Multivariate Data Analyses." R Package., 2020.
25. Husson, F.; Josse, J.; Le, S.; Mazet, J. Package 'FactoMineR,' 2020.
26. Rai, A.; Sharma, V.; Heitholt, J. Dry Bean [*Phaseolus Vulgaris* L.] Growth and Yield Response to Variable Irrigation in the Arid to Semi-Arid Climate. *Sustainability* **2020**, *12* (9), 3851. https://doi.org/10.3390/su12093851.
27. Wan, L.; Li, Y.; Cen, H.; Zhu, J.; Yin, W.; Wu, W.; Zhu, H.; Sun, D.; Zhou, W.; He, Y. Combining UAV-Based Vegetation Indices and Image Classification to Estimate Flower Number in Oilseed Rape. *Remote Sensing* **2018**, *10* (9), 1484. https://doi.org/10.3390/rs10091484.

28. Zhang, S.; Zhang, H.; Di, B.; Song, L. Cellular UAV-to-X Communications: Design and Optimization for Multi-UAV Networks. *IEEE Transactions on Wireless Communications* **2019**, *18* (2), 1346–1359. https://doi.org/10.1109/TWC.2019.2892131.
29. Meyer, G. E.; Neto, J. C. Verification of Color Vegetation Indices for Automated Crop Imaging Applications. *Computers and Electronics in Agriculture* **2008**, *63* (2), 282–293. https://doi.org/10.1016/j.compag.2008.03.009.
30. Bendig, J.; Yu, K.; Aasen, H.; Bolten, A.; Bennertz, S.; Broscheit, J.; Gnyp, M. L.; Bareth, G. Combining UAV-Based Plant Height from Crop Surface Models, Visible, and near Infrared Vegetation Indices for Biomass Monitoring in Barley. *International Journal of Applied Earth Observation and Geoinformation* **2015**, *39*, 79–87. https://doi.org/10.1016/j.jag.2015.02.012.
31. Huete, A. R. A Soil-Adjusted Vegetation Index (SAVI). *Remote Sensing of Environment* **1988**, *25* (3), 295–309. https://doi.org/10.1016/0034-4257(88)90106-X.
32. Woebbecke, D. M.; Meyer, G. E.; Von Bargen, K.; Mortensen, D. A. Shape Features for Identifying Young Weeds Using Image Analysis. *Transactions of the American Society of Agricultural Engineers* **1995**, *38* (1), 271–281.
33. Lussem, U.; Bolten, A.; Gnyp, M. L.; Jasper, J.; Bareth, & B. Lussem, U., Bolten, A., Gnyp, M. L., Jasper, J., & Bareth, G. (2018). Evaluation of RGB-Based Vegetation Indices from UAV Imagery to Estimate Forage Yield in Grassland. Int. Arch. Photogramm. Remote Sens. Spatial Inf. Sci, 42(3), 1215-1219. **2018**, *42* (3), 1215–1219.
34. Yeom, J.; Han, Y.; Kim, T.; Kim, Y. Forest Fire Damage Assessment Using UAV Images : A Case Study on Goseong-Sokcho Forest Fire in 2019. 한국측량학회지 **2019**, *37* (5), 351–357.
35. Beniaich, A.; Naves Silva, M. L.; Avalos, F. A. P.; Menezes, M. D.; Candido, B. M. Determination of Vegetation Cover Index under Different Soil Management Systems of Cover Plants by Using an Unmanned Aerial Vehicle with an Onboard Digital Photographic Camera. *Semina-Ciencias Agrarias* **2019**, *40* (1), 49–66.
36. Jin, X.; Liu, S.; Baret, F.; Hemerlé, M.; Comar, A. Estimates of Plant Density of Wheat Crops at Emergence from Very Low Altitude UAV Imagery. *Remote Sensing of Environment* **2017**, *198*, 105–114. https://doi.org/10.1016/j.rse.2017.06.007.
37. Bareth, G.; Bendig, J.; Tilly, N.; Hoffmeister, D.; Aasen, H.; Bolten, A. A Comparison of UAV- and TLS-Derived Plant Height for Crop Monitoring: Using Polygon Grids for the Analysis of Crop Surface Models (CSMs). *undefined* **2016**.
38. Hashimoto, N.; Saito, Y.; Maki, M.; Homma, K. Simulation of Reflectance and Vegetation Indices for Unmanned Aerial Vehicle (UAV) Monitoring of Paddy Fields. *Remote Sensing* **2019**, *11* (18), 2119. https://doi.org/10.3390/rs11182119.
39. Saberioon, M. M.; Cisar, P. Automated Multiple Fish Tracking in Three-Dimension Using a Structured Light Sensor. *Computers and Electronics in Agriculture* **2016**, *121*, 215–221. https://doi.org/10.1016/j.compag.2015.12.014.
40. Freden, S. C.; Mercanti, E. P.; Becker, M. A. *Third Earth Resources Technology Satellite-1 Symposium: Section A-B. Technical Presentations*; Scientific and Technical Information Office, National Aeronautics and Space Administration, 1974.
41. Kemerer, C. F.; Slaughter, S. A. Determinants of Software Maintenance Profiles: An Empirical Investigation. *Journal of Software Maintenance: Research and Practice* **1997**, *9* (4), 235–251. https://doi.org/10.1002/(SICI)1096-908X(199707/08)9:4<235::AID-SMR153>3.0.CO;2-3.
42. Li, Y.; Chen, D.; Walker, C. N.; Angus, J. F. Estimating the Nitrogen Status of Crops Using a Digital Camera. *Field Crops Research* **2010**, *118* (3), 221–227. https://doi.org/10.1016/j.fcr.2010.05.011.
43. Hu, L.; Pan, H.; Zhou, Y.; Zhang, M. METHODS TO IMPROVE LIGNIN'S REACTIVITY AS A PHENOL SUBSTITUTE AND AS REPLACEMENT FOR OTHER PHENOLIC COMPOUNDS: A BRIEF REVIEW. *BioResources* **2011**, *6* (3), 3515–3525.